Eur. Phys. J. B **36**, 141–147 (2003)
DOI: 10.1140/epjb/e2003-00327-8

THE EUROPEAN PHYSICAL JOURNAL B

Mixing length scales: step meandering and island nucleation on vicinal surfaces

M. Rusanen[1,2,a], I.T. Koponen[2], and J. Kallunki[3,b]

[1] Laboratory of Physics, PO Box 1100, 02015 HUT, Espoo, Finland
[2] Department of Physical Sciences, University of Helsinki, PO Box 64, 00014 University of Helsinki, Finland
[3] Fachbereich Physik, Universität Essen, 45117 Essen, Germany

Received 9 April 2003
Published online 19 November 2003 –

Abstract. Simultaneous island nucleation and step flow growth on vicinal surfaces are studied by Monte Carlo simulations. Step edges experience meandering instability under growth conditions if there is a kink barrier suppressing adatom jumps around kink sites. This instability has a characteristic length scale, with different scaling properties from the island separation scale. We show that there is a coupling between island nucleation and step edge instability. The length scale associated with nucleation begins to couple with the wavelength of the step edge patterns when islands and steps coalesce. Only in the submonolayer regime step meandering is independent of island formation. In this regime the island separation has a cross-over scaling behaviour as terrace width is varied.

PACS. 81.15.Aa Theory and models of film growth – 68.55.Ac Nucleation and growth: microscopic aspects – 81.16.Rf Nanoscale pattern formation

1 Introduction

Growth patterns on surfaces have recently attracted considerable interest, mainly as a promising possibility to directly produce nanoscale structures through surface growth kinetics [1,2]. The advents in atomic resolution imaging techniques have revealed many previously unknown features and details of growth on patterned surfaces [3,4]. The experimental progress has revived modelling and theoretical efforts to better understand the basic atomistic processes and regularities behind the pattern formation.

At present, on vicinal (stepped) surfaces much is known about the conditions required for smooth layer-by-layer growth. The dynamics and atomistic processes at step edges, and scaling and morphology of growing patterns are well-known issues, although some details remain unresolved [5,6]. Moreover, the additional kink crossing barrier, which is the cause of the kink Ehrlich-Schwoebel effect (KESE) [7], is recognised to be of the major importance for meandering instability at close-packed step edges [7–12]. On the other side, on singular (flat) surfaces island growth during submonolayer deposition has been extensively studied [13,14] because of its importance for further growth [15,16]. In particular, the interlayer processes and the associated Ehrlich-Schwoebel barriers [17] are of central importance for obtaining smooth layer-by-layer growth [1,2]. Currently both on vicinal and singular surfaces the development and the scaling properties of the associated length scales characterizing growth are well known.

During real surface growth an interesting and rather common situation is that both step flow and island nucleation have effects on growth. The importance of this regime has been noted already on studies devoted to fairly idealized growth conditions [2,18], but thus far it has not received much attention (see, however, Refs. [19–23]). The basic problem is the complicated interplay between step flow and island nucleation. Since they both have unique scaling properties arising spontaneously from the dynamics of the growth processes, the competition between two growth modes becomes complicated. On vicinal surfaces meandering instability due to KESE produces step edge patterns which have a certain characteristic length scale on close-packed step edges [10–12]. On the other hand, in island growth the natural length scale can be associated with the mean distance between the islands [24]. When these elementary growth modes and their dynamics are operative at the same time, it is far from obvious whether one of them and the associated length scale begins to dominate over the other. It is also possible that an effective length scale, the same for both growth modes, appears together with new features in surface growth. As a result,

[a] *Present address:* Institut Français du Pétrole, Groupe de Modélisation Moléculaire, BP 311, 92852 Rueil-Malmaison, France; e-mail: `Marko.Rusanen@ifp.fr`
[b] *Present address:* Laboratory of Physics, PO Box 1100, FIN–02015 HUT, Espoo, Finland

this new length scale could have scaling properties and/or quantitative values different from the elementary growth modes.

In order to clarify the above stated problem connected to competition between island growth and step flow, we utilize Monte Carlo simulations on two-dimensional fcc surfaces using semi-realistic energy barriers. The advantage of our approach is that both island processes [25] and step meandering [11,26] have been addressed previously with the same method. In both cases good agreement with experimental results has been obtained, indicating that essential features of the both isolated growth modes are treated in a reasonable way. Based on these previous studies, we show here by simulations that coalescence between growing islands and advancing steps couples island nucleation and the step edge pattern formation during deposition. This is indicated by quantitative changes in both length scales, in the island separation and the wavelength of the edge patterns. For small fluxes these length scales saturate as a function of coverage and for high fluxes exhibit oscillations around the mean values. In the submonolayer regime the scaling of the meander wavelength is independent of island nucleation on terraces. In this case, scaling of the island density shows a cross-over behavior when the terrace width is varied, a result previously found in reference [19].

2 Competing growth modes: step meandering and island growth

In order to gain understanding of simultaneous step meandering and island growth, we briefly review the basic notions of interest in both cases separately. It is well known, that smooth step flow growth on a vicinal surface is maintained when adatoms landing on terraces attach to preexisting step edges before they nucleate new islands (dimers) with other adatoms. However, the step morphology changes due to the additional energy barrier (Ehrlich-Schwoebel barrier [17]) suppressing interlayer mass transport. This is the so-called Bales-Zangwill (BZ) instability, where straight steps are morphologically unstable against long wavelength fluctuations [18,27,28].

Recently it has been noted that the meandering of steps may be caused also by another instability mechanism due to the kink Ehrlich-Schwoebel barrier [7], which could supersede the BZ instability. If there is an extra barrier for an atom to cross a corner site at the step edge (e.g. on a close-packed step edge [29]), a destabilizing mass current in the up-kink direction appears [7], a one-dimensional analog of mound formation on singular surfaces [30]. This picture has been shown to agree with the Monte Carlo simulations based on the semi-realistic description of energy barriers and the surface structure [11], in the case of more simplified solid-on-solid model [12], and it is also consistent with the experiments [10]. The wavelength of the step edge meandering originates from a process, where adatoms attaching to the step edge preferentially migrate along the edge [29] and eventually at the edge, dimers are nucleated. Dimers grow to larger protrusions when more adatoms attach to the edge. Because adatoms attach more likely to these small protrusions, unstable growth results. Therefore, for KESE the stabilization of step edge patterns is inherently related also to dimer nucleation at the edge [11], which is reflected in the scaling properties of the meanders [11,12]. The notion that the meander wavelength λ is determined by dimer nucleation at the step edge leads to the prediction [31,32]:

$$\lambda \approx \ell_d \sim \left(\frac{D_s}{F_s}\right)^{1/4}, \tag{1}$$

where ℓ_d is the dimer nucleation length in one dimension, $D_s \propto \exp[-E_d/k_BT]$ is the adatom diffusion coefficient and E_d is the diffusion barrier along the straight edge, $F_s = FL$ is the flux onto the edge, and L is the terrace width. The patterns have a well-defined wavelength, which does not depend on coverage after the initial transient regime [11]. The saturation of λ already at the early stage of growth indicates the crucial role of dimer nucleation. In the case of pattern formation during step flow growth, the scaling form given by equation (1) is valid from the submonolayer coverage up to several monolayers (ML), if island formation on terraces is suppressed [11,12].

The regularities in growth instability caused by KESE suggest that island nucleation on a vicinal surface during step flow could produce interesting features. Island nucleation is assumed to be rather insensitive to the presence of the step edges in the submonolayer stage and on large enough terraces. However, when surface coverage increases during deposition, steps and islands begin eventually to coalesce. Due to the coalescence between steps and islands, the number density of islands abruptly changes. Moreover, coalescence of islands with steps lead to protrusions at the edges that changes available terrace area for nucleation. This would ultimately affect not only the length scale of island separation but also the length scale of step edge patterns.

For islands, on a singular surface, the relevant length scale is determined by the typical distance between islands ℓ_n, which is set during submonolayer deposition. Incoming adatoms nucleate new islands, since in the initial stage of growth there are no steps or islands present where newly landed adatoms could attach. Nucleation terminates when a saturation regime is reached, and all incoming adatoms attach to already existing islands. Consequently, the total number of islands remains constant. If one assumes stable and immobile dimers, the nucleation length on a singular surface is given by [24]

$$\ell_n \sim (D/F)^{1/6}. \tag{2}$$

When island growth is operative on terraces of a vicinal surface, it must be noted that the terrace width L appears also as a length scale. If L is much larger than ℓ_n, growth proceeds as on a singular surface. On a terrace with smaller L most adatoms attach to the step edge and only few islands appear [19]. On a vicinal surface in the limit of large terraces $L \gg \ell_n$ in the submonolayer regime, the island density N (number of islands per

unit area) is supposed to scale as on a singular surface, $N = \ell_n^{-2} \sim (F/D)^{1/3}$, where D is the adatom diffusion coefficient. As the terrace width decreases adatoms attach preferentially to steps instead of nucleating new islands. If L is small enough (step-dominated nucleation), only one island fits between the edges of neighbouring steps. Following the arguments in references [2,24,32] one obtains the nucleation length of the islands (see Appendix) on a small terrace as

$$\tilde{\ell}_n \sim \frac{D}{FL^5}, \tag{3}$$

and consequently the island density in this regime is given by $\tilde{N} = 1/(\tilde{\ell}_n L) \sim FL^4/D$. Setting the expressions for the island densities equal, $N = \tilde{N}$, results for a crossover value of the flux $F_c = D/L^6$, or the terrace width $L_c = (D/F)^{1/6}$. By appropriately scaling the island density gives the expression

$$N \sim L^{-2} \begin{cases} f & \text{for } f \ll 1; \\ f^{1/3} & \text{for } f \gg 1, \end{cases} \tag{4}$$

where $f = F/F_c$. This result agrees with reference [19], apart from a slightly different L-dependence. Our scaling form is based on a simple argument for the nucleation length, whereas in reference [19] a self-consistent treatment of the island capture numbers is used.

In the submonolayer regime where the island density has not yet saturated one can define the effective island density as [13,33] $N_{\text{eff}} \sim (\theta F/D)^{\gamma}$. We apply this to equation (4) obtaining the prediction

$$N_{\text{eff}} = L^{-2}(\theta f)^{\gamma}, \tag{5}$$

where $\gamma = 1$ in step-dominated nucleation and $\gamma = 1/3$ on a singular surface, as described above. During the nucleation period the distance between islands decreases until the saturation of the density is reached. Since in our simulations on a vicinal surface the saturation regime during submonolayer deposition is seldom reached we will use equation (5) in what follows.

3 Model

In our Monte Carlo model atoms are randomly deposited onto a vicinal surface, where they randomly migrate, attach to or detach from steps and islands, or nucleate a new island with other adatoms. At every lattice site the surface has a single-valued height, i.e. overhangs are not permitted. If an atom is deposited onto a overhang position it is relaxed down-hill until a single-valued site is found. Adatoms are allowed to jump only to the nearest-neighbor sites.

The simulations were performed on fcc(1,1,m) ($m = 19 - 81$) surfaces which are vicinal to fcc(001). These surfaces consist of (001) terraces separated by the close-packed [110] step edges. The system sizes were $L_x = 1000$, in the units of the lattice constant ($L_x = 3000$ for the smallest fluxes) in the direction of steps and $L_y = 74-162$ in the perpendicular direction depending on terrace width. The simulations were implemented using the BKL algorithm [34] with the periodic boundary conditions in the direction of steps and helical boundary conditions in the direction of vicinality. For the energy barriers of atomistic jumps the values based on EMT description on a Cu surface were used [29] with the prefactor 3×10^{12} s^{-1}. These energy barriers follow a simple bond counting scheme, where the barrier for transition between two states is determined by the difference between the neighboring bonds in the final and the initial states. For completeness, the Ehrlich-Schwoebel barrier at the step edge was also included in the model. However, this would not be necessary to observe the KESE instability [11,12]. Figure 1 shows a schematic picture of the step edge on a fcc vicinal surface with some typical processes and their energy barriers used in the model.

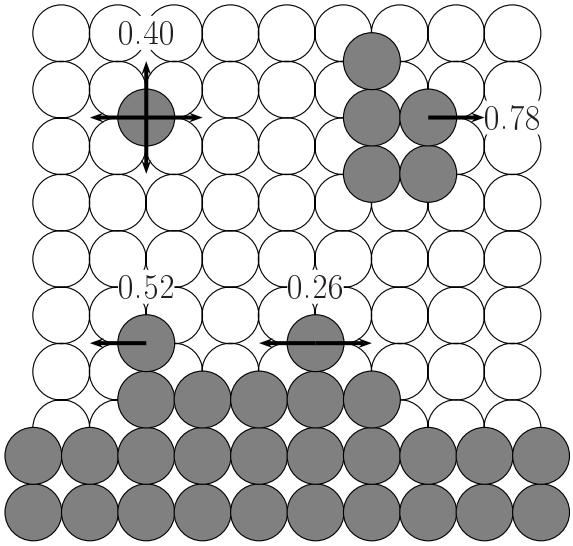

Fig. 1. A schematic picture of the terrace and the step edge on a fcc surface viewed above with some typical processes indicated as arrows. Solid circles correspond to the upper and open circles the lower terrace, respectively. The numbers denote the energy barriers in the units of eV.

4 Results

Simulations were carried out at the temperature $T = 240$ K in the submonolayer regime and $T = 200-240$ K in multilayer deposition for fluxes $F = 5.0 \times 10^{-2} - 5.0$ ML/s typically in the coverage range $\theta = 0 - 3$ ML. With these choices island nucleation is operative with the terrace widths $L \geq 9$.

Some representative snapshots of surface configurations are displayed in Figure 2 with the terrace width $L = 12$, the flux $F = 0.1$ ML/s, and temperature $T = 240$ K at coverages a) $\theta = 0.2$ ML, b) 2.0 ML, and c) 6.0 ML. The step profiles are shown with the solid line, adatoms as black circles, and for clarity only the center-of-mass positions of terrace islands are indicated as black squares. Only

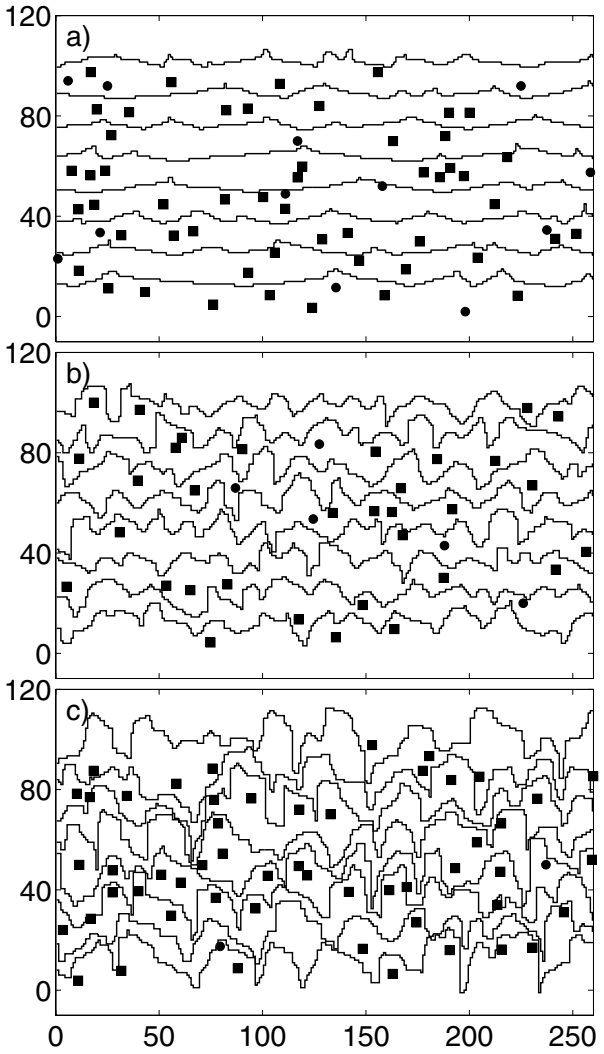

Fig. 2. The snapshots of some surface configurations are shown. The solid lines are the step profiles, the black circles denote the adatoms, and the black squares mark the center-of-mass positions of the islands. The surface is fcc(1,1,25) with $L = 12$. Other parameters are $T = 240$ K, $F = 0.1$ ML/s, and a) $\theta = 0.2$ ML, b) 2.0 ML, and c) 6.0 ML. Axis are given in the units of the lattice constant. Note the different scales in horizontal and vertical directions. In the submonolayer regime the step edge morphology and the wavelength are independent of nucleation events. When coverage increases coalescence of step edges and islands begins resulting changes in λ and ℓ_n.

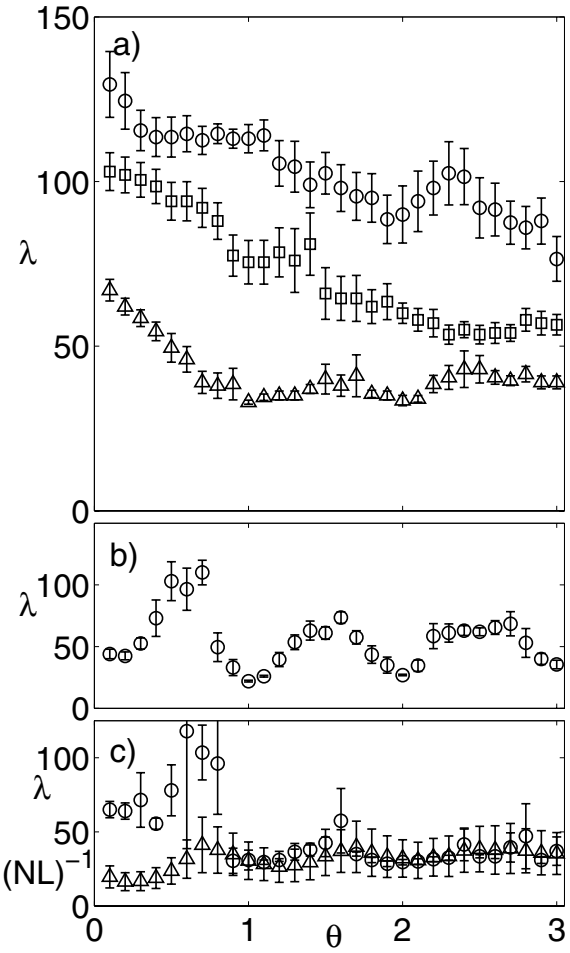

Fig. 3. a) displays the meander wavelength λ (in the units of the lattice constant) versus coverage in the range $\theta = 0-3$ ML with parameters $T = 240$ K, $F = 5 \times 10^{-2} - 10^{-1}$ ML/s from top to bottom. λ approaches a saturation value after an initial period; b) shows λ with $F = 1.0$ ML/s at $T = 220$ K. For large fluxes and/or low temperatures λ shows oscillations around the mean value as a function of coverage. In this regime defect creation might also play a role; c) shows a comparison between λ (circles) and the island separation scale on a small terrace $\tilde{\ell}_n = (NL)^{-1}$ (triangles) with $F = 0.75$ ML/s and $T = 240$ K. Large errors in the island separation are due to small number of islands on terraces. However, the scales are of the same order within the errors.

the one-to-one mappings of the step profiles are shown, since the real profiles have many overhangs in the profile curve due to coalescence between islands and steps. From the snapshots it is evident that for small coverages islands and step patterns grow independently until island coalescence with edges begins roughly after $\theta \approx 0.3$ ML. When an island becomes a part of the edge, the step morphology changes and at the same time the step locally advances instantaneously ahead. The protrusions caused by the coalesced island relax rather rapidly thus removing overhangs from the step profiles, except for the highest fluxes. For high fluxes edge relaxation is slow compared with the advancement of the step. This produces overhangs into the step edge profiles leading eventually to nucleation of vacancy islands on terraces.

Figures 3a and b display the behavior of the meander wavelength λ as a function of coverage in the range $\theta = 0-3$ ML with a) $T = 240$ and $F = 5 \times 10^{-2} - 10^{-1}$ ML/s, and b) $T = 220$ K with $F = 1.0$ ML/s. We define λ through the relation $\lambda = 4y_0$, where y_0 is the position of the first zero of the step profile correlation function. The correlation function is defined as $C(y) = \langle [x(y) - x(0)]^2 \rangle$, where $x(y)$ is the step profile. For small fluxes λ decreases from the predicted value without island nucleation given

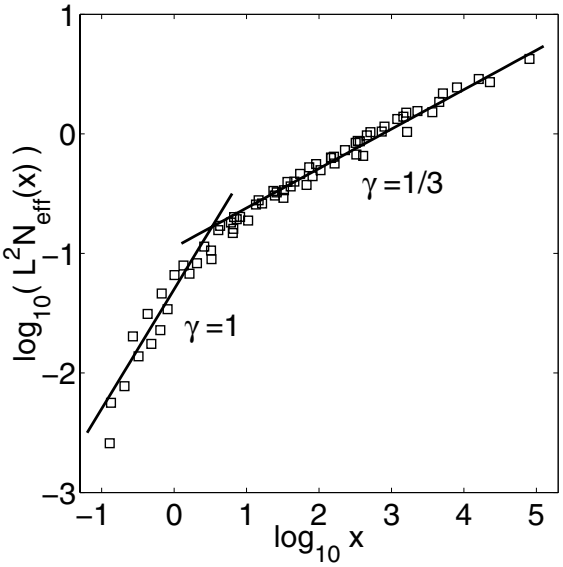

Fig. 4. The scaled island density $L^2 N_{\rm eff}(x)$ is displayed as a function of the scaling parameter $x = \theta F/F_c$. The solid lines correspond to the power law $L^2 N_{\rm eff}(x) \sim x^\gamma$ (see Eq. (5)). The data consist of densities obtained from different terrace widths between $L = 8 - 40$ and submonolayer coverages in the range $\theta = 0.0 - 0.3$ ML. The scatter in the data is of the order of statistical errors. For small argument values the data follow step-dominated nucleation and after the cross-over at $F = F_c$ obey singular surface scaling.

by equation (1) until it attains a saturation value λ_s. The saturation value decreases as the flux increases. If the flux is large enough or temperature low, λ saturates quickly and oscillates around λ_s. In Figure 3c the island separation scale $\tilde{\ell}_n$ on a small terrace is compared with the meander wavelength with $T = 240$ K and $F = 0.75$ ML/s. The scales reach the saturation value close to $\theta = 1.0$ ML. However, the errors in $\tilde{\ell}_n$ are relatively large due to rather a small number of islands on small terraces.

In Figure 4 the scaled island density $L^2 N_{\rm eff}(x)$ is displayed as a function of the scaling variable $x = \theta F/F_c$ in the submonolayer regime (up to $\theta = 0.3$ ML for small and $\theta = 0.1$ ML for large L). At small x the scaled density the data follows scaling of the step-dominated regime and at large x that of the singular surface, both regimes comprised in equation (5). There is a cross-over between these two regimes around $F \approx F_c$. This demonstrates that in the submonolayer regime before coalescence between islands and steps, island nucleation and step flow are independent growth modes.

5 Discussion

A realistic description of surface growth includes both step flow and island nucleation on terraces. A non-vanishing barrier for adatoms to cross corner sites at the steps will ultimately result to meandering instability (KESE) on close-packed step edges with a dynamically selected wavelength. On the other hand, on terraces there is another length scale set by the island separation. In the submonolayer regime there is no essential coupling between island nucleation and step flow, since coalescence between islands and steps does not occur. Thus the length scales are different with unique scaling properties. The situation changes when growth proceeds beyond the submonolayer stage, since for large coverages island formation is coupled with step flow through coalescence between islands and steps. As a result, the step edge morphology, the associated meander wavelength, and also the mean island separation will change. Our results suggest that in this growth regime both length scales approach values of the same order and after a transient stage a new characteristic scale is reached, presumably the same for both growth modes.

The onset of the effective length scale in the case of simultaneous island formation and meandering, demonstrated in Figure 3, and its regularities can be understood by (but not derived from) the scaling properties of the isolated growth modes. The new scale is clearly qualitatively different from the original meander wavelength λ and the island separation on small terraces $\tilde{\ell}_n$. The results show that there is a coupling between λ and $\tilde{\ell}_n$ such that they both deviate from their submonolayer values, where scaling with respect to D/F (Eqs. (1) and (5)) is valid. The origin of that change is twofold. Firstly, step morphology changes due to coalescence of islands with advancing steps. Secondly, at the same time the step edges inevitably change the island separation and the available terrace area for island nucleation.

For small fluxes both λ and $\tilde{\ell}_n$ approach the flux-dependent saturation values. If the flux is large, the length scales saturate rather rapidly and oscillate around the flux-independent mean values. These oscillations could indicate alternating nucleation and step flow where λ and $\tilde{\ell}_n$ periodically change as growth proceeds. However, close to the maxima of λ the step profiles have the largest fluctuations in shapes and amplitudes. This is reflected in the errors of the correlation function, which are the largest at the maxima. For large fluxes the profiles have many overhangs due to irregular shapes of coalescing islands, which causes errors in the calculation of the correlation function. For large fluxes vacancy nucleation and other defect creation (e.g. second layer nucleation on top of terrace islands) also affect the step profiles.

The advantage of the semi-realistic simulations carried out here is mainly to demonstrate convincingly that the development of the effective length scale due to the competition between the elementary growth modes is really an outcome of the atomistic processes. We can reliably rule out the possibility, that it is an artifact of the method or model simplifications, which could easily happen in more simplified scenarios. Moreover, the choice of the semi-realistic energy barriers in the simulations makes it possible to establish a connection between the scaling properties of the effective length scale and scaling properties of the elementary growth modes. This provides us the necessary results needed for further simplifications of the model in order to distinguish the essential atomistic

processes from the irrelevant ones. For example, we have explicitly checked that if the diffusion barrier along the edge is increased to the same value as the barrier for terrace diffusion, quantitative changes in the meander wavelength do not occur. The drawback of the semi-realistic simulations is the relatively long computation times needed to reach the stationary regime, where island growth and step meandering are competing processes. Within reasonable computation time we are able to simulate up to $\theta = 5$ ML. There is an indication that λ and ℓ_n maintain the saturation values up to 10 ML (not shown here) for certain parameter combinations. However, in order to study quantitatively scaling properties of the effective length scale, its temperature dependence, and stationary profile shapes at large coverages in more detail, better statistics is needed. The current simulations could not rule out the possibility that the effective length scale has the same scaling properties as one of the elementary growth modes, only with the different prefactor.

6 Conclusions

Island nucleation coupled with step meandering on vicinal surfaces have been studied by kinetic Monte Carlo simulations. In the submonolayer regime the island density has a cross-over scaling as a function of the terrace width and flux. In this regime, the growth modes and the associated length scales are shown to be independent. At larger coverages there is always a coupling between island nucleation and step flow leading to mixing of the length scales. This is indicated by qualitative changes in the meander wavelength and the island separation scale as coverage increases. The both scales ultimately saturate to the flux-dependent values of the same order. The coupling has been shown to be essentially due to coalescence of growing islands with advancing step edges. The intriguing feature of the mixing length scales is their astonishing regularity and emergence of a new well defined effective scale with the saturation value of the same order, but yet essentially different from those of the isolated processes.

The results suggest that the interesting coupling between island nucleation and step meandering during step flow growth on vicinal surfaces could lead to entirely new kind of scaling properties of growing patterns. This would indicate that there could be more possibilities to manipulate the step edge patterns by island nucleation than previously believed only on the basis of the elementary processes. Our results are therefore of importance for interpreting experiments involving step meandering and island nucleation, and for constructing more realistic models of surface growth.

Helpful suggestions and discussions with T. Ala-Nissila and J. Krug are gratefully acknowledged. This research has been supported by Academy of Finland, project 73642. M.R. thanks also Vaisala Foundation for travel support.

Appendix: Derivation of ℓ_n in the step-dominated regime

Consider a rectangular area $\ell \times L$ on a vicinal surface (terrace width L). Steps dominate nucleation when $L < \ell_n$ since most adatoms attach to step edges instead of nucleating new islands. In this regime only one island on the average fits between the neighboring edges. Following the arguments of references [2,24,32] there are $F\ell L$ adatoms landing on the terrace region of size $\ell \times L$ and an adatom visits L^2 sites on the average (apart from logarithmic corrections, and setting the lattice constant equal to one). Nucleation probability per unit time at the length ℓ is then given by

$$P(\ell) = F\ell L L^2 \langle \rho \rangle, \tag{6}$$

where $\langle \rho \rangle$ is the average adatom concentration on a terrace (equal to the probability that a site is occupied).

The continuous adatom concentration obeys the diffusion equation in the perpendicular direction of steps [35], $\partial_t \rho = D\partial_{xx}\rho + F$. The boundary conditions are $\rho(0) = \rho(L) = 0$ when assuming for simplicity complete adatom sticking at the edges and no Ehrlich-Schwoebel barrier. In the stationary limit $\partial_t \rho \approx 0$, and the average concentration becomes [24] $\langle \rho \rangle \approx \frac{F}{D} L^2$. Inserting this into equation (6) and setting the probability for nucleation $P(\tilde{\ell}_n)/F \approx 1$ gives $\tilde{\ell}_n \approx (D/F)L^{-5}$. One obtains for the island density the scaling form:

$$\tilde{N} = \frac{1}{\tilde{\ell}_n L} \approx \frac{F}{D} L^4. \tag{7}$$

The cross-over between step-dominated and singular surface nucleation can be found by equating this expression with the singular surface result, which applies for $L \gg \tilde{\ell}_n$. This leads to the cross-over value for the flux $F_c = D/L^6$.

References

1. H.-C. Jeong, E.D. Williams, Surf. Sci. Rep. **34**, 171 (1999)
2. P. Politi, G. Grenet, A. Marty, A. Ponchet, J. Villain, Phys. Rep. **324**, 271 (2000)
3. H. Brune, Surf. Sci. Rep. **31**, 121 (1998)
4. P. Finnie, Y. Homma, Surf. Sci. **500**, 437 (2002)
5. J. Kallunki, J. Krug, Phys. Rev. E **62**, 6229 (2000)
6. F. Gillet, O. Pierre-Louis, C. Misbah, Eur. Phys. J. B **18**, 519 (2000)
7. O. Pierre-Louis, M.R. D'Orsogna, T.L. Einstein, Phys. Rev. Lett. **82**, 3661 (1999)
8. T. Salditt, H. Spohn, Phys. Rev. E **47**, 3524 (1993)
9. M.V. Ramana Murty, B.H. Cooper, Phys. Rev. Lett. **83**, 352 (1999)
10. T. Maroutian, L. Douillard, H.-J. Ernst, Phys. Rev. Lett. **83**, 4353 (1999); Phys. Rev. B **64**, 165401 (2001)
11. M. Rusanen, I.T. Koponen, J. Heinonen, T. Ala-Nissila, Phys. Rev. Lett. **86**, 5317 (2001)
12. J. Kallunki, J. Krug, M. Kotrla, Phys. Rev. B **65**, 205411 (2002)
13. M.C. Bartelt, J.W. Evans, Phys. Rev. B **46**, 12675 (1992)
14. G.S. Bales, D.C. Chrzan, Phys. Rev. B **50**, 6057 (1994)

15. R. Kunkel, B. Poelsema, L.K. Verheij, G. Comsa, Phys. Rev. Lett. **65**, 733 (1990)
16. P. Šmilauer, M.R. Wilby, D.D. Vvedensky, Phys. Rev. B **47**, 4119 (1993)
17. G. Ehrlich, F.G. Hudda, J. Chem. Phys. **44**, 1039 (1966); R.L. Schwoebel, E.J. Shipsey, J. Appl. Phys. **37**, 3682 (1966)
18. G.S. Bales, A. Zangwill, Phys. Rev. B **41**, 5500 (1990); Phys. Rev. B **48**, 2024 (1993)
19. G.S. Bales, Surf. Sci. **356**, L439 (1996)
20. A.K. Myers-Beaghton, D.D. Vvedensky, Phys. Rev. B **42**, 9720 (1990); Phys. Rev. A **44**, 2457 (1991); V. Fuenzalida, Phys. Rev. B **44**, 10835 (1991); S. Kenny, M.R. Wilby, A.K. Myers-Beaghton, D.D. Vvedensky, Phys. Rev. B **46**, 10345 (1992)
21. S. Harris, Surf. Sci. **424**, L335 (1999); Surf. Sci. **453**, L315 (2000)
22. S. Clarke, D.D. Vvedensky, Phys. Rev. Lett. **58**, 2235 (1987); J. Appl. Phys. **63**, 2272 (1988)
23. A. Pimpinelli, P. Peyla, Int. J. Mod. Phys. B **11**, 3647 (1997)
24. J. Villain, A. Pimpinelli, L. Tang, D. Wolf, J. Phys. I France **2**, 2107 (1992)
25. J. Heinonen, I. Koponen, J. Merikoski, T. Ala-Nissila, Phys. Rev. Lett. **82**, 2733 (1999)
26. M. Rusanen, I.T. Koponen, T. Ala-Nissila, C. Ghosh, T.S. Rahman, Phys. Rev. B **65**, 041404 (2002)
27. L. Schwenger, R.L. Folkerts, H.-J. Ernst, Phys. Rev. B **55**, R7406 (1997)
28. M. Rost, P. Šmilauer, J. Krug, Surf. Sci. **369**, 393 (1996)
29. J. Merikoski, I. Vattulainen, J. Heinonen, T. Ala-Nissila, Surf. Sci. **387**, 167 (1997); J. Merikoski, T. Ala-Nissila, Phys. Rev. B **52**, 8715 (1995)
30. J. Villain, J. Phys. I France **1**, 19 (1991)
31. J. Krug, M. Schimschak, J. Phys. I France **5**, 1065 (1995)
32. P. Politi, J. Phys. I France **7**, 797 (1997)
33. D.E. Wolf, in *Scale invariance, interfaces, and non-equilibrium dynamics*, edited by M. Droz, A.J. McKane, J. Vannimenus, D.E. Wolf (Plenum, New York 1994), pp. 215–248
34. A.B. Bortz, M.H. Kalos, J.L. Lebowitz, J. Comput. Phys. **17**, 10 (1975); M. Kotrla, Comput. Phys. Commun. **97**, 82 (1995); J.L. Blue, I. Beichl, F. Sullivan, Phys. Rev. E **51**, 867 (1995)
35. W.K. Burton, N. Cabrera, F.C. Frank, Phil. Trans. R. Soc. London, Ser. A **243**, 299 (1951)